

Synthesis and optical properties of iron(III) complexes of 2-benzylidene-1-indanone derivative thin films†

Cite this: *J. Mater. Chem. C*, 2014, 2, 5607

M. Lozano González,^a M. E. Sánchez-Vergara,^{*b} J. R. Álvarez-Bada,^b M. I. Chávez-Uribe,^a Rubén A. Toscano^a and C. Álvarez-Toledano^{*a}

In this work, we propose a different method to synthesize 2-benzylidene-1-indanone derivatives and a new method to obtain iron(III) complexes of 2-benzylidene-1-indanone derivatives, used to prepare semiconducting thin films. The 2-benzylidene-1-indanone derivatives were obtained from the reaction of *o*-phthalaldehyde with acetophenone in a basic medium and were later complexed with Fe₂(CO)₉ to form iron(III) complexes from the corresponding redox reaction. One of the iron complexes (**4a**) was fully characterized by single-crystal X-ray diffraction. Iron(III) complexes of 1-indenol derivative thin films were obtained by thermal evaporation in a high vacuum source. All the samples were grown at room temperature (25 °C) and low deposition rates (0.2 Å s⁻¹) on quartz substrates and (100) single-crystalline silicon (c-Si) wafers. The surface morphology and structure of the deposited films were studied by atomic force microscopy (AFM) and scanning electron microscopy (SEM). Optical absorption studies of the iron(III) complex films were performed in the 100–1150 nm wavelength range. The optical band gap (*E*_g) of the thin films was determined from the $(\alpha h\nu)^{1/2}$ vs. $h\nu$ plots for indirect allowed transitions. The iron(III) complex films show optical activation energies around 2.1 eV, depending on the 1-indenol derivative. From these results, iron complexes of 1-indenol derivatives may prove suitable for photovoltaic or luminescence applications.

Received 24th March 2014
Accepted 7th May 2014

DOI: 10.1039/c4tc00599f

www.rsc.org/MaterialsC

Introduction

The search for new materials for optoelectronic applications has led to an ever increasing interest in organometallics and organic compounds. Compounds combining different organometallic moieties and their electron transfer processes have attracted a considerable amount of attention.^{1–3} Organometallic compounds may eventually be considered for electronic applications requiring a large area coverage, structural flexibility and low-temperature processing.^{4–6} Recent research work has been oriented to the formation and characterization of semiconducting thin films. Some methods have been extensively used to produce organometallic semiconducting thin films, such as chemical vapor deposition, electrodeposition and vacuum thermal evaporation.⁷ Research on the production of films with transition metal complexes has particular relevance, due to the

oxidation states of transition metals by the electron transfer processes. Metal chelates are one of these transition metal complexes that are widely used as building blocks in modern organic synthesis. A thorough understanding of their structure and reactivity is important because many of these compounds exist as aggregates in solutions and in the solid state. Depending on the metal and organic building blocks, they can possess properties such as luminescence, catalytic capability and other material chemical features.⁸ These metal chelates with oxygen atoms, such as β -diketones, can form transition metal complexes with atoms like gadolinium that show interesting luminescent properties.⁸ Other organic building blocks worthy of consideration are 2-hydroxyphenone, indenols and 2-benzylidene-1-indanones.

There are spectroscopic investigations of arylidene derivatives that show that an increase in the electron interactions of electron-donor substituents in a conjugated bond system leads to some kind of flattening of the molecules,⁹ so this feature in 2-benzylidene-1-indanone is an interesting structural characteristic for materials chemistry applications. As far as we are aware, there are no reports of this phenomenon involving the preparation of semiconducting thin films with iron.

1-Indanone compounds are important synthetic intermediates for pharmaceutical agents and biologically active compounds, and there are numerous methods available for the

^aInstituto de Química, Universidad Nacional Autónoma de México, Circuito Exterior Ciudad Universitaria, 04510, México, D. F., Mexico

^bUniversidad Anáhuac del Norte, Avenida Universidad Anáhuac, núm. 46, Col. Lomas Anáhuac, C.P. 52786, Huixquilucan, Estado de México, Mexico. E-mail: elena.sanchez@anahuac.mx

† Electronic supplementary information (ESI) available: NMR and mass spectrometry data are provided in the attached files. CCDC 992714 and 992715. For ESI and crystallographic data in CIF or other electronic format see DOI: 10.1039/c4tc00599f

preparation of 1-indanones.^{10a} Akio Saito *et al.* described their synthesis with catalytic SbF_5 and the use of EtOH to convert a mixture of phenylalkynes and aldehydes to indanone compounds in one pot.^{10a} The benzylidene-1-indanone derivatives have many conjugated unsaturated linkages, so they are versatile building blocks for many compounds, such as pharmaceuticals, agrochemicals and perfumes, new organic materials for nonlinear optical applications, cytotoxic analogs, and units of liquid-crystalline polymers.^{10b} Many molecules of this type are synthesized from aldehydes and cycloalkanones. Yu Wan *et al.* synthesized α, α' -bis(substituted-benzylidene)cycloalkanones *via* a solvent-free cross-aldol condensation of aromatic aldehydes with cycloalkanones in the presence of a catalytic amount of 1-methyl-3(2-(sulfoxy)ethyl)-1*H*-imidazol-3-ium chloride at room temperature and showed their optical properties.^{10c} Camille Carrignon *et al.* obtained α, α' -bis(substituted-benzylidene)cycloalkanone derivatives using chloride ion pairs as catalysts for the alkylation of aldehydes and ketones with C–H acidic compounds.^{10d}

In this work, we propose an easier and faster method to synthesize 2-benzylidene-1-indanone derivatives and a new method to synthesize iron(III) complexes of 2-benzylidene-1-indanone derivatives. Thin films of these complexes were prepared by thermal evaporation and characterized by scanning electron microscopy (SEM), atomic force microscopy (AFM) and infrared spectroscopy (IR). We also report the determination of optical parameters related to the main transitions in the UV-vis region, as well as the fundamental energy gap calculations for these films.

Results and discussion

In this work, we used carbonyl-substituted 2-benzylidene-1-indanone, *o*-phthalaldehyde and aryl-substituted methyl ketones with a sodium hydroxide ethanolic solution at room temperature, which provided good yields and a faster reaction. To understand the influence of different substituents in this type of compounds in the presence of $\text{Fe}_2(\text{CO})_9$, 2-benzylidene-1-indanone derivatives were synthesized according to the reaction shown in Fig. 1.

The IR spectra of the substituted 2-benzylidene-1-indanone derivatives 1–4 showed the characteristic absorption assigned to the C=O group vibrations near 1700 cm^{-1} , and the absence of absorption in the $\nu(\text{O–H})$ region of the 2-benzylidene-1-

indanone spectrum was considered evidence that the free ligand is a proton chelate and therefore exists largely in the chelated enol form.¹¹ The analysis of the NMR spectroscopic data (^1H , ^{13}C , COSY, HSQC and HMBC experiments) allowed to discern between the two possible enolic forms (Fig. 2a and b), according to the location of the double bond (endocyclic or exocyclic to the ring B) in solution (Fig. 2).

The 1H and 2D COSY experiments showed a characteristic AA'BB' system which corresponded to the hydrogen atoms H-1, H-2, H-3 and H-4 of ring A, and a second aromatic system was assigned to the hydrogen atoms H-10 to H-14 for ring C. At 3.8–3.9 ppm a singlet resonated which integrated for two hydrogens that were assigned to H-15a and b of ring B. The HSQC experiments allowed the identification of the corresponding carbons linked to the hydrogens described above, confirming the assignments. In the ^{13}C spectra for compound 1 and for compounds 2–4, three and four signals of quaternary aromatic carbons were observed, respectively. These were assigned to C-5, C-16 of ring A and C-9 and C-12 of ring C, since HMBC correlations were observed (Fig. 3) between H-2 and C-16, between H-3 and C-5, and between H-10, H-11, H-13 and H-14 with C-9 and C-12. Finally, long range HMBC correlations established the location of the double bond at C7–C8 for compounds 1–4, according to the following observations: the aromatic hydrogen H-4 displayed a HMBC cross-peak with the carbonyl C-6 (194.5–196 ppm); the aromatic hydrogen H-1 correlated with the methylene C-15, and the aromatic hydrogens H-10 and H-14 correlated with the olefinic carbon C-8. The same correlations were observed for compounds 1–4, confirming the structures.

Crystals suitable for the X-ray structure determination of compound 1 were grown from a mixture of *n*-hexane and dichloromethane solution that confirmed the structure proposed (Fig. 4). 1 crystallizes in the space group $Pna2_1$ with two symmetry independent molecules in the unit cell, A and B. In both symmetry independent molecules, the C–O bonds of carbonyl 1.274(14) and 1.16(3) and hydroxyl 1.437(19) and 1.35(2) show a good differentiation of both moiety groups that correlates with the RMN experiments. The crystal forms a two-dimensional, hydrogen-bonded (O–H \cdots O) network, which is parallel to the plane, and the enol form is stabilized through intramolecular hydrogen bonding. Details of the collected crystallographic data are provided in the ESI.†

These results show that the generalization made by Brown is correct in this case: “Double bonds which are *exo* to a 5-ring are less reactive and more stable than related double bonds which

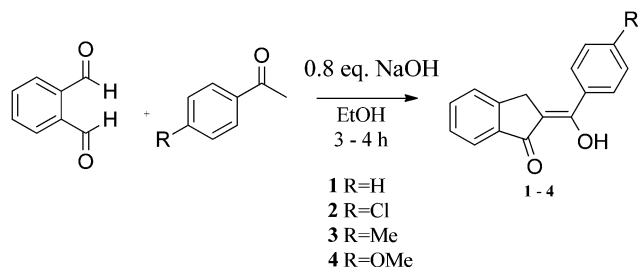


Fig. 1 Synthesis of 2-benzylidene-1-indanone derivative compounds 1 to 4.

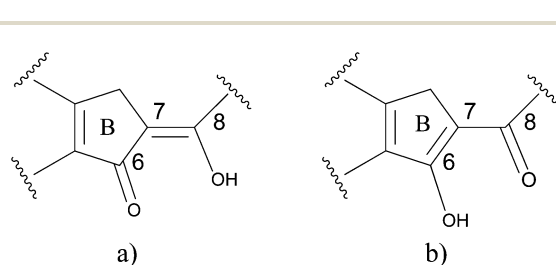


Fig. 2 (a) Exocyclic double bond, 2-benzylidene-1-indanone-type and (b) endocyclic double bond, 1-indenol-type.

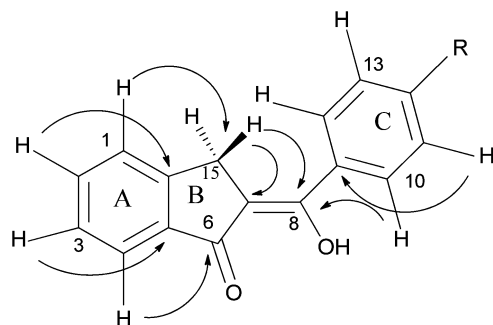


Fig. 3 HMBC correlations of 1 to 4.

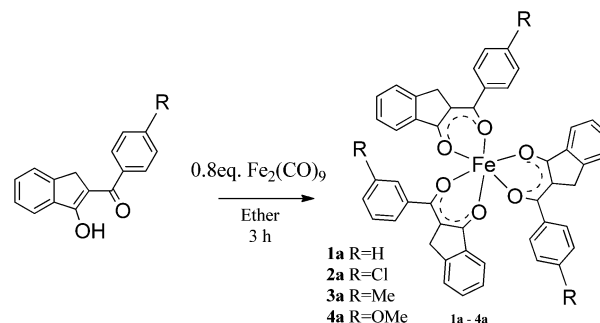


Fig. 5 Synthesis of iron complexes of 2-benzylidene-1-indanone derivative compounds 1a to 4a.

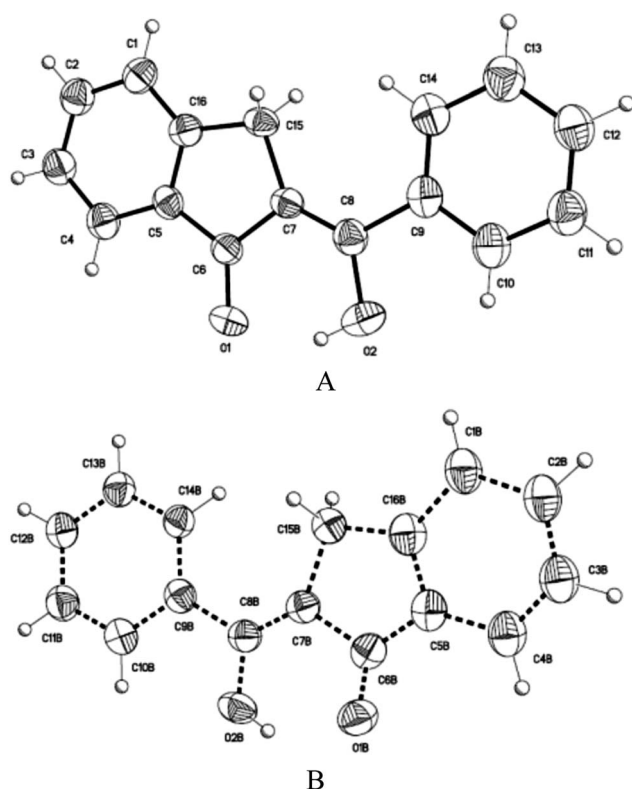


Fig. 4 ORTEP plot of the two symmetry-independent molecules of 1. Atomic labels are shown for the asymmetric units and hydrogen atoms have been omitted for clarity.

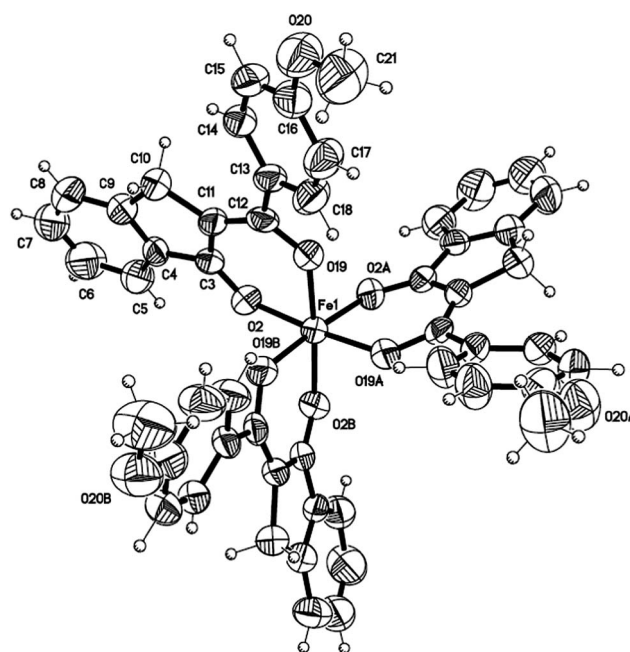


Fig. 6 ORTEP drawing, with omission of hydrogen atoms, of the complex 4a.

are *exo* to a 6-ring. Reactions which involve the formation or retention of an *exo* double bond in a 5-ring derivative will be favored over corresponding reactions which involve the formation or retention of an *exo* double bond in a 6-ring derivative".¹²

A suspension of ligands 1–4 and $\text{Fe}_2(\text{CO})_9$ in anhydrous ether (Fig. 5) led to the formation of 1a–4a, which were isolated by filtration. As far as we are aware, there are no reports on the synthesis of 1a–4a by other methods. Paramagnetic complexes 1a, 2a, 3a, and 4a were obtained as violet, deep red and black crystalline solids.

Crystals suitable for the X-ray structure determination of 4a were grown from a mixture of *n*-hexane and dichloromethane solution (Fig. 6). Details of the collected crystallographic data

are provided in the ESI.† Complex 4a crystallizes in the space group $R\bar{3}$. The molecular structure is shown in Fig. 3 and confirms the suggested structure. The units show a distorted octahedral arrangement (Table 1), with the *trans* O–Fe–O angles of $175.07(11)^\circ$, and very similar *cis* O–Fe–O angles which fall in the range $86.75(11)$ – $92.53(11)^\circ$. The corresponding Fe–O distances of hydroxyl (1.98 Å) and carbonyl are very similar (1.99 Å). This arrangement follows a trend that was observed in

Table 1 Selected interatomic distances (Å) and angles ($^\circ$) for 4a

Bond	(Å)	Angle	($^\circ$)
Fe1–O19	1.983 (3)	O19–Fe1–O19 (1)	88.45 (11)
Fe–O2	1.999 (3)	O19(1)–Fe1–O2	175.08 (11)
O2–C3	1.281 (4)	O19–Fe1–O2	86.75 (11)
O2–C2	1.297 (4)	O19–Fe1–O2 (1)	92.53 (10)
		O19–Fe1–O2 (2)	175.07 (11)

some complexes formed by iron(III) with salicylate-based tripodal ligands.¹³ The rest of the synthesized compounds (**1a**–**3a**) are expected to have a similar crystalline structure because the only change in the compound refers to the radical of the iron complex.

IR analysis shows some similarities in the IR spectrum absorption bands for the compounds **1a** to **4a** (see Table 2). The absence of absorption in the 1700 cm^{-1} region was construed as evidence that coordination occurs through the enol tautomer. Features in the region around 1580 – 1600 cm^{-1} were attributable to the carbonyl bond $\nu(\text{C}=\text{O})$, that is shifted to lower frequencies; this and the presence of the band around 1550 cm^{-1} , attributable to the C–O bond of increased single-bond order, were consistent with a cyclic structure for the metal complexes with coordination through both carbonyl groups.¹³

After deposition of the thin films, a comparison of the IR absorption spectra of the synthesized complexes and those of the deposited films indicated that thermal evaporation is a good technique to obtain iron complexes of 2-benzylidene-1-indanone derivative thin films.⁸ Iron(III) in 2-benzylidene-1-indanone derivatives can form complexes with strong metal–ligand covalent bonds, which enhance molecular stability and support the sublimation process without dissociation.⁸ The IR measurements were performed on films deposited over monocrystalline silicon substrates. There are a few differences between signals identified on powder materials and those deposited on films, and they may be due to internal stress produced during the vaporization process.

The variations in the microscopic morphology and roughness of the films deposited onto quartz substrates were examined by atomic force microscopy and are shown in Fig. 7 and Table 3. 3D micrographs provide a large surface inspection of the micro-structural arrays, topological structure, porosity and film quality of the deposited layers. Thin films from samples **1a**, **2a** and **4a** (Fig. 7a, b and d) show a very similar aspect. The films are extremely homogeneous and a fine granular structure can be observed in them. In the case of the film from sample **3a**, a heterogeneous distribution is seen and particles agglomerate to generate irregular structures (Fig. 7c). The calculated RMS wrinkle heights for the thin films are shown in Table 3. This evaluation was performed on three different sites. The difference in the roughness values may be related to the different iron(III) complexes of 2-benzylidene-1-indanone derivatives in each thin film. Less roughness is found in the compound with

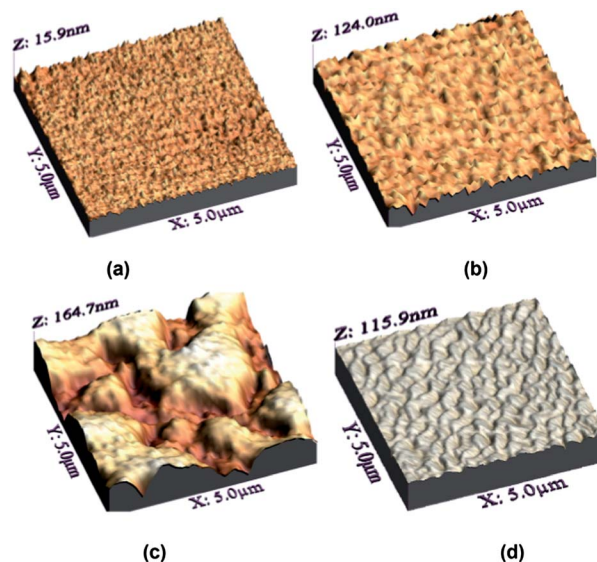


Fig. 7 3D-micrographs obtained by AFM, showing the surface morphology of thin films deposited on quartz slices from the: (a) **1a** thin film, (b) **2a** thin film, (c) **3a** thin film and (d) **4a** thin film, respectively.

Table 3 AFM evaluation of the thin film roughness, thickness and optical activation energy

Compound	RMS roughness (nm)	Film thickness (Å)	Indirect optical activation energy (eV)
1a	1.29	959	2
2a	29.06	1527	2.1
3a	33.45	1233	2.1
4a	4.57	3632	2.1

hydrogen **1a** and in the complex **4a** with the methoxy group, while thin film **2a** with Cl and thin film **3a** containing the methyl group as a substituent are the roughest. In fact, compound **3a**, with the methyl group, produces the most heterogeneous and roughest thin film, followed by compound **2a**, with the chloride anion. The methyl- and chloride-containing compounds seem to have been most affected by the thermal gradient occurring between the room-temperature substrate and the high-temperature evaporated material, which nucleated upon the substrate and then completely covered it during the sublimation process. IR spectroscopy results suggest that the compounds did not undergo chemical decomposition (Table 2) and had similar deposition rates. Nevertheless, they showed – as thin films – morphological differences that depended directly on the substituent radical and the electrostatic forces occurring during deposition.

The SEM micrographs in Fig. 8 show the surface morphologies of iron(III) complexes of 2-benzylidene-1-indanone derivatives; notice the small domains. Fig. 8a, b and d show micrographs at $1000\times$ corresponding to the **1a**, **2a** and **4a** thin films, respectively. From these figures, it is clear that the evaporation process (with the substrate at 323 K) produced homogeneous thin films. In the $1000\times$ micrograph of the **3a** thin film

Table 2 IR (cm^{-1}) characteristic bands for powder and thin films

Compound	$\nu(\text{C}=\text{O})\text{ cm}^{-1}$	$\nu(\text{C}-\text{O})\text{ cm}^{-1}$
1a (pellet)	1587	1553
1a (thin film)	1584	1552
2a (pellet)	1582	1551
2a (thin film)	1580	1553
3a (pellet)	1585	1546
3a (thin film)	1582	1550
4a (pellet)	1599	1547
4a (thin film)	1595	1549

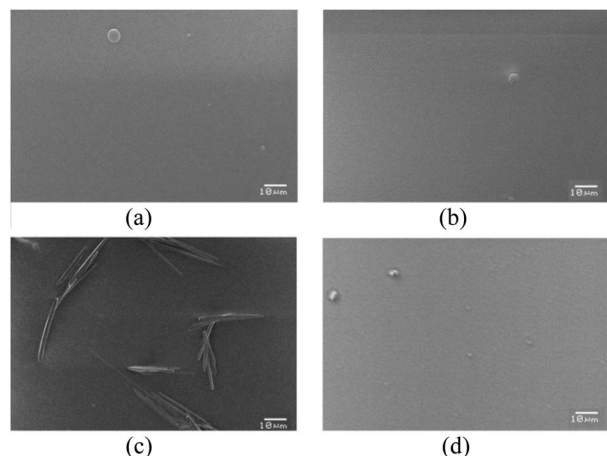


Fig. 8 SEM micrographs of materials (a) **1a**, (b) **2a**, (c) **3a** and (d) **4a**, at 1000 \times .

(Fig. 8c), one can readily find two apparent phases. One phase shows a coating with elongated crystals and the second one is the homogeneous phase. Although this film was grown at room temperature and low deposition rates, we observe a significant contribution of the bulk crystalline phase, with seemingly preferential directions for crystal nucleation and growth. This effect may be attributed to the higher thickness of the thin film.⁵ Table 3 shows thickness values for all thin films. It is worth noting that the most heterogeneous deposition, as well as the roughest thin film, corresponds to the compound having a methyl functional group in its molecule. This film feature seems to be a consequence of its particular crystal growth.

UV spectra of iron(III) complexes of 2-benzylidene-1-indanone derivatives show high-intensity bands arising from electronic transitions in the conjugated system (see Fig. 9a). The iron(III) complexes of 2-benzylidene-1-indanone derivatives have absorption bands in the UV-visible region assigned to the following electronic transitions: (i) d-d transitions arising from ligand field interactions, (ii) intraligand transitions ($\pi \rightarrow \pi^*$) arising from molecular orbitals localized in the ligand and (iii) charge transfer transitions (LMCT or MLCT) involving an electron transition from the ligand to the metal ion or from the metal ion to the ligand, respectively.⁸ An intense band appearing in the near-ultraviolet region (228–241 nm) seems to

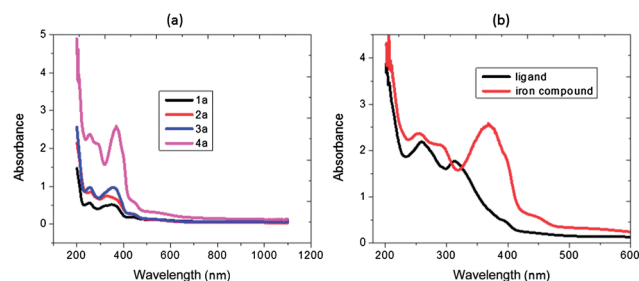


Fig. 9 (a) UV spectra of iron(III) complexes of 2-benzylidene-1-indanone derivatives and (b) UV spectra of ligand and iron compounds **4** and **4a**.

correspond to a $\pi \rightarrow \pi^*$ transition in the enolate ring⁸ and the one at 276–297 nm comes from $\pi \rightarrow \pi$ and $\pi \rightarrow \pi^*$ intraligand transitions. The band around 410–422 nm is due to charge transfer from the ligand to the metal ion.⁸ The π interaction in the enolate ring is influenced by the type of ligand substituent.¹⁴ Fig. 9b shows the UV-vis ligand and complex spectra. The absence of the signal at about 400 nm in the ligand spectrum is readily noticed, suggesting substantial changes in electron mobility arising from the addition of the metallic ions. From the obtained absorption values, use of these films as photo-conducting materials and in color filters may be considered.¹⁵

The value of the absorption coefficient (α) of iron(III) complexes of 2-benzylidene-1-indanone derivative thin films is calculated at different energies and plotted in Fig. 10a. Up to about 3 eV, α has a similar value in all the compounds. This may be due to the absorption coefficient explicitly depending on the electronic structure of the metal ion. The peak at the UV threshold indicates the contribution of the d-electrons of the iron(III) to the electronic transitions.^{16a,b} For higher energy values, however, the **3a** thin film (the one with methyl) has the largest α value, while the **2a** film (the one with chloride) has the smallest α value. The methyl group's electronic density and the film's heterogeneity also affect the material's optical behavior at higher photon energies ($h\nu$). Notice, however, that thin-film optoelectronic applications frequently involve $h\nu$ values smaller than 2 eV. To obtain information on direct or indirect inter-band transitions, the fundamental absorption edge data were analyzed within the framework of one-electron theory^{16a,b} and according to the relationship:

$$\alpha = \alpha_0(h\nu - E_g)^r$$

E_g is the optical band gap, and r determines the type of transitions, with $r = 2$ and 3 for allowed and forbidden indirect transitions and $r = 1/2$ and $3/2$ for allowed and forbidden direct transitions. The dependence of $(\alpha)^{1/r}$ on photon energy ($h\nu$) was evaluated and plotted for different values of r , and the best fit was obtained for $r = 2$. This characteristic behavior corresponds to allowed indirect transitions;^{16a,b} the optical band gap is determined from the intercept on the energy axis of the linear fit of the larger energy data, in a plot of $(\alpha h\nu)^{1/2}$ vs. $h\nu$ (Tauc extrapolation¹⁷), as shown in Fig. 10b. The optical gap for **1a–4a** was found to be in the range 2–2.1 eV (see Table 3), corresponding to wavelengths of 590–620 nm in the electromagnetic

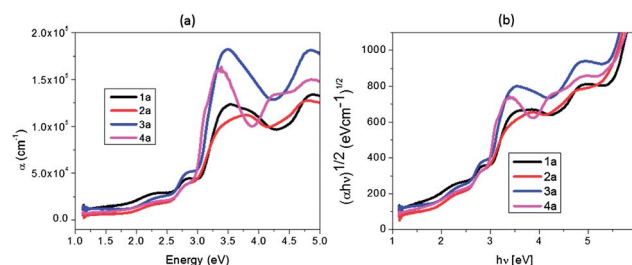


Fig. 10 (a) Energy dependence of the absorption coefficient (α) of iron(III) complexes of 2-benzylidene-1-indanone derivative thin films and (b) plot of $(\alpha/h\nu)^{1/2}$ vs. photon energy $h\nu$.

spectrum. The non-direct electronic transitions seem to be of the π to π^* type. In these electronic transitions, occurring from states of the valence band to states of the conduction band, there is no conservation of the electronic momentum.¹⁸ The optical activation energy values are very similar in all the compounds. The ligand does not seem to influence electronic transport between the valence and conduction bands of these compounds, the metallic center being responsible for conductivity. From these results, iron(III) complexes of 2-benzylidene-1-indanone derivatives may prove suitable for photovoltaic¹⁸ or luminescence applications,⁸ as well as in dyes and pigments. Their semiconductor-like properties may also permit their use in sensors and molecular electronics applications. As the metallic ion and its oxidation state are the main drivers of the optical properties in these thin films, the effect of other metallic atoms in the ligand needs to be understood in order to better establish a specific application for these materials. Work with complexes involving other metals has now been undertaken and will be published later on.

Experimental

All reagents and solvents were obtained from commercial suppliers and used without further purification. $\text{Fe}_2(\text{CO})_9$ was synthesized from $\text{Fe}(\text{CO})_5$ according to the literature.¹² All compounds were characterized by IR spectra, recorded on a Perkin-Elmer 283B or 1420 spectrophotometer, by the KBr technique, and all data are expressed in wavenumbers (cm^{-1}). Melting points were obtained on a Melt-Temp II apparatus and are uncorrected. Nuclear magnetic resonance spectra were recorded with a Bruker AV 400 or JEOL Eclipse +300 spectrometer. Chemical shifts for the ^1H NMR spectra were recorded in parts per million from tetramethylsilane with the solvent resonance as the internal standard (chloroform, $\delta = 7.25$ ppm). Chemical shifts for the ^{13}C NMR spectra were recorded in parts per million from tetramethylsilane using the central peak of CDCl_3 ($\delta = 77.1$ ppm) as the internal standard. Mass spectra were recorded with a JEOL JMSAX 505 HA spectrometer at 70 eV using the electronic impact (EI) and fast atom bombardment (FAB^+) technique. A suitable X-ray quality crystal of one of the iron complexes (**4a**) was grown by slow evaporation of an *n*-hexane- CH_2Cl_2 mixture at room temperature. The crystal was mounted on a glass fiber at room temperature, and then placed on a Bruker Smart Apex CCD diffractometer, equipped with Mo $\text{K}\alpha$ radiation; decay was negligible. Structure solutions and refinements were performed using SHELXTL V6.10.¹⁹

General procedure for the synthesis of 2-benzylidene-1-indanone derivatives

The reaction between *o*-phthalaldehyde and acetophenone in a basic medium was performed to produce the 2-benzylidene-1-indanone type compound under simpler and faster conditions. *o*-Phthalaldehyde was added slowly to a cool sodium hydroxide (0.8 eq.) ethanolic solution with the appropriate amount of acetophenone. The reaction mixture was stirred at room temperature for approximately 3 h, and then poured into a

mixture of ice and commercial hydrochloric acid (pH was adjusted to about 7). The resulting solid was filtered and in some cases purified by column chromatography using hexane/ethyl acetate.

Compound 1. ($\text{C}_{16}\text{H}_{12}\text{O}_2$, $M = 236$ g mol $^{-1}$) was prepared starting from *o*-phthalaldehyde (0.5 g, 3.7 mmol), acetophenone (0.48 g, 3.7 mmol) and NaOH (0.119 g, 2.98 mmol) and was obtained as a yellow solid, mp. 90 °C, (0.67 g, 2.82 mmol, 75%). IR: ν 1604, 1564 cm^{-1} . ^1H NMR (300 MHz, CDCl_3): $\delta = 15.067$ (s, 1H, OH), 7.49, 7.5 (d, 1H, 1), 7.54 (ddd, 1H, 2), 7.40 (dd, 1H, 3), 7.85 (d, 1H, 4), 7.91 (m, 1H, 10), 7.48 (m, 3H, 11, 12, 13), 7.91 (m, 1H, 14), 3.86 (sa, 2H, 15) ppm. ^{13}C NMR (75 MHz, CDCl_3): $\delta = 125.54$ (C1), 133.27 (C2), 127.40 (C3), 123.36 (C4), 137.85 (C5), 195.70 (C6), 109.41 (C7), 170.79 (C8), 134.79 (C9), 128.07 (C10), 128.55 (C11), 131.21 (C12), 128.55 (C13), 128.07 (C14), 32.19 (C15), 148.51 (C16) ppm. MS (EI): m/z (%) = 236 (1.9%). HRMS (FAB^+): calculated for $\text{C}_{16}\text{H}_{12}\text{O}_2$: 237.0821. Found: 237.0823.

Compound 2. ($\text{C}_{16}\text{H}_{11}\text{ClO}_2$, $M = 270.5$ g mol $^{-1}$) was prepared starting from *o*-phthalaldehyde (0.5 g, 3.7 mmol), 4'-chloroacetophenone (0.58 g, 3.7 mmol) and NaOH (0.119 g, 2.98 mmol) and was obtained as a pale brown solid, mp. 162–164 °C, (0.8 g, 2.96 mmol, 80%). IR: ν 1605, 1559 cm^{-1} . ^1H NMR (300 MHz, CDCl_3): $\delta = 15.03$ (s, 1H, OH), 7.54 (d, 1H, 1), 7.60 (d, 1H, 2), 7.44 (ddd, 1H, 3), 7.86 (dd, 1H, 4), 7.89 (d, 2H, 10, 14), 7.48 (d, 2H, 11, 13), 3.91 (s, 2H, 15) ppm. ^{13}C NMR (75 MHz, CDCl_3): $\delta = 125.45$ (C1), 133.35 (C2), 127.35 (C3), 123.19 (C4), 137.44 (C5), 195.63 (C6), 109.29 (C7), 169.14 (C8), 132.99 (C9), 129.22 (C10), 128.70 (C11), 137.22 (C12), 128.70 (C13), 129.22 (C14), 31.95 (C15), 148.19 (C16) ppm. MS (EI): m/z (%) = 270 (15%). HRMS (FAB^+): calculated for $\text{C}_{16}\text{H}_{11}\text{ClO}_2$: 271.0526. Found: 271.0522.

Compound 3. ($\text{C}_{17}\text{H}_{14}\text{O}_2$, $M = 250$ g mol $^{-1}$) was prepared starting from *o*-phthalaldehyde (0.5 g, 3.7 mmol), 4'-methylacetophenone (0.5 g, 3.7 mmol) and NaOH (0.119 g, 2.98 mmol) and was obtained as a yellow solid, mp. 96–98 °C, (0.71 g, 2.84 mmol, 76%). IR: ν 1604, 1540 cm^{-1} . ^1H NMR (300 MHz, CDCl_3): $\delta = 15.17$ (s, 1H, OH), 7.50 (d, 1H, 1), 7.55 (ddd, 1H, 2), 7.41 (dd, 1H, 3), 7.85 (d, 1H, 4), 7.84 (d, 1H, 10), 7.30 (d, 2H, 11, 13), 7.84 (d, 1H, 14), 3.89 (sa, 2H, 15), 2.41 (s, 3H, 17) ppm. ^{13}C NMR (75 MHz, CDCl_3): $\delta = 125.50$ (C1), 133.11 (C2), 127.35 (C3), 123.27 (C4), 137.95 (C5), 195.45 (C6), 109.01 (C7), 171.09 (C8), 131.97 (C9), 128.08 (C10), 129.29 (C11), 141.89 (C12), 129.29 (C13), 128.08 (C14), 32.32 (C15), 148.39 (C16), 21.52 (C17) ppm. MS (EI): m/z (%) = 250 (20%). HRMS (FAB^+): calculated for $\text{C}_{17}\text{H}_{14}\text{O}_2$: 251.1072. Found: 251.1079.

Compound 4. ($\text{C}_{17}\text{H}_{14}\text{O}_3$, $M = 266$ g mol $^{-1}$) was prepared starting from *o*-phthalaldehyde (0.5 g, 3.7 mmol), 4'-methoxyacetophenone (0.56 g, 3.7 mmol) and NaOH (0.119 g, 2.98 mmol) and was obtained as a yellow solid, mp. 112–114 °C, (0.7 g, 2.6 mmol, 71%). IR: ν 1601, 1566 cm^{-1} . ^1H NMR (300 MHz, CDCl_3): $\delta = 15.33$ (s, 1H, OH), 7.47 (d, 1H, 1), 7.51 (dd, 1H, 2), 7.37 (dd, 1H, 3), 7.82 (d, 1H, 4), 7.89 (d, 2H, 10, 14), 6.95 (d, 2H, 11, 13), 3.82 (s, 2H, 15), 3.83 (s, 3H, 17) ppm. ^{13}C NMR (75 MHz, CDCl_3): $\delta = 125.37$ (C1), 132.85 (C2), 127.23 (C3), 123.03 (C4), 137.87 (C5), 194.84 (C6), 108.32 (C7), 170.04 (C8), 127.00 (C9), 129.99 (C10), 113.88 (C11), 162.06 (C12), 113.88 (C13), 129.99 (C14), 32.45 (C15), 148.09 (C16), 55.30 (C17) ppm. MS (EI): m/z

(%) = 266 (15%). HRMS (FAB⁺): calculated for C₁₇H₁₄O₃: 267.1021. Found: 267.1023.

General procedure for the synthesis of iron(III) complexes of 2-benzylidene-1-indanone derivatives

A solution of 2-benzylidene-1-indanone derivatives (compounds 1 to 4) in anhydrous ethyl ether (20 mL) was treated with Fe₂(CO)₉ at room temperature for 2–3 h, under an inert atmosphere (Fig. 2). After the reaction was complete, the crude product was filtered off through a Celite column, washed with ethyl ether and dissolved in dichloromethane. The solvent was evaporated to dryness. The iron complex(III) was obtained in a pure form.

Compound 1a. (C₄₈H₃₃FeO₆, *M* = 761 g mol^{−1}) was prepared starting from 2-(phenylmethanone)-inden-1-ol (0.5 g, 2.1 mmol), and Fe₂(CO)₉ (0.31 g, 0.85 mmol) and was obtained as a purple solid, mp. 244–246 °C, (0.425 g, 0.558 mmol, 80%). MS (FAB⁺): *m/z* (%) = 761 (2%). HRMS (FAB⁺): calculated for C₃₂H₂₂O₄Fe [M⁺]: 526.0867. Found: 526.0877.

Compound 2a. (C₄₈H₃₀Cl₃FeO₆, *M* = 863 g mol^{−1}) was prepared starting from 2-(4-chlorophenylmethanone)-inden-1-ol (0.5 g, 1.85 mmol), and Fe₂(CO)₉ (0.27 g, 0.74 mmol) and was obtained as a purple solid, mp. 232–234 °C, (0.48 g, 0.55 mmol, 90%). MS (FAB⁺): *m/z* (%) = 864 (2%). HRMS (FAB⁺): calculated for C₃₂H₂₀O₄ClFe [M⁺]: 594.0088. Found: 594.0092.

Compound 3a. (C₅₁H₃₉FeO₆, *M* = 803 g mol^{−1}) was prepared starting from 2-(4-methylphenylmethanone)-inden-1-ol (0.5 g, 2 mmol), and Fe₂(CO)₉ (0.29 g, 0.8 mmol) and was obtained as a purple solid, mp. 238–240 °C, (0.33 g, 0.4 mmol, 61%). MS (FAB⁺): *m/z* (%) = 803 (5%). HRMS (FAB⁺): calculated for C₃₄H₂₆O₄Fe [M⁺]: 554.1180. Found: 554.1187.

Compound 4a. (C₅₁H₃₉FeO₉, *M* = 851 g mol^{−1}) was prepared starting from 2-(4-methoxyphenylmethanone)-inden-1-ol (0.5 g, 1.87 mmol), and Fe₂(CO)₉ (0.274 g, 0.75 mmol) and was obtained as a purple solid, mp. 234–236 °C, (0.37 g, 0.43 mmol, 70%). MS (FAB⁺): *m/z* (%) = 851 (2%). HRMS (FAB⁺): calculated for C₃₄H₂₆O₆Fe [M⁺]: 586.1079. Found: 554.1082.

Thin film deposition and characterization

Thin film deposition of iron(III) complexes with substituted 2-benzylidene-1-indanones was carried out by vacuum thermal evaporation. The material was deposited onto quartz and (100) single-crystalline silicon (c-Si) 200 Ω cm wafers. The substrate temperatures were kept at 298 K during deposition. The evaporation source was a tungsten boat and the temperature through the tungsten boat was slowly increased to 498 K. The pressure in the vacuum chamber before the film deposition was 1 × 10^{−6} Torr and the evaporation rate was 0.2 Å s^{−1}. The thickness measurements were made with a Sloan Dektak IIA profilometer on a quartz substrate. IR measurements were performed with a Nicolet iS5-FT spectrophotometer, using silicon flakes as a substrate for the thin films. For SEM, a Leica Cambridge scanning electron microscope (model Stereoscan 440) was coupled to a microanalysis system and operated at a voltage of 20 kV and a focal distance of 25 mm, using thin films on a quartz substrate. AFM characterization was performed

using a JEOL microscope, model JSPM-4210, with the Tapping (AFM) work mode. For AFM characterization of the films, quartz substrates were used. Ultraviolet-visible spectroscopy was carried out using a Unicam spectrophotometer, model UV300, with a quartz substrate.

Conclusions

We show an easy and fast method to synthesize 2-benzylidene-1-indanone derivatives and a new method to synthesize iron(III) complexes of 2-benzylidene-1-indanone derivatives, used to prepare semiconducting thin films. Thin films were prepared by a vacuum thermal evaporation process. The thermal evaporation process had no effect on the intra-molecular bonds, suggesting that the chemical composition of the films did not change. The thin-film morphology seems to depend on the molecular structure. The chemical differences between the substituents in the complexes and the structural variations observed in the molecular-film arrangements provided a glimpse of the optical properties of these compounds. The optical transitions were found to be of non-direct nature. The optical band gap was calculated and the values found were similar among all thin films. The optical absorption coefficients of iron(III) complexes of 2-benzylidene-1-indanone derivatives, as well as their optical band gaps, makes their thin films promising candidates for potential applications in solar cells or as emitting layers in OLEDs.

Acknowledgements

The authors wish to thank the technical assistance of M. Rivera (IF-UNAM), Rocío Patiño, Luis Velasco, Javier Pérez and IN4 (IQ-UNAM), as well as Guillermo Villagrán (Universidad Anáhuac). The authors gratefully acknowledge the financial support of the SEP-CONACYT-México, under the project number 153751 and the CONACYT project 127796 and the DGAPA-PAPIIT project IN207414. We would also like to thank the CONACYT for the Ph.D. grant extended to M. L. G.

Notes and references

- 1 S. Rigaut, J. Massue, D. Touchard, J. L. Fillaut, S. Golhen and P. H. Dixneuf, *Angew. Chem., Int. Ed.*, 2002, **41**, 4513.
- 2 J. C. Röder, F. Meyer and E. Kaiser, *Angew. Chem., Int. Ed.*, 2002, **41**, 2304.
- 3 D. Astruc, *Acc. Chem. Res.*, 1997, **30**, 383.
- 4 R. A. Laudise, C. Kloc, P. G. Simpkins and T. Siegrist, *J. Cryst. Growth*, 1998, **187**, 449.
- 5 J. Puigdollers, C. Voz, A. Orpella, I. Martin, M. Vetter and R. Alcubilla, *Thin Solid Films*, 2003, **427**, 367.
- 6 M. E. Sánchez-Vergara, A. Ortiz, C. Álvarez-Toledano, J. G. López-Cortés, A. Moreno and J. R. Álvarez, *Thin Solid Films*, 2008, **516**, 6382.
- 7 P. Cassoux, D. De Caro, L. Valade, H. Casellas, B. Daffos and M. E. Sánchez Vergara, *Mol. Cryst. Liq. Cryst.*, 2002, **380**, 45.
- 8 J. Zabicky, *The Chemistry of Metal Enolates*, Part 1 (Patai Series), Wiley, England, 2009.

- 9 (a) V. Orlov, I. Borovoi and V. F. Lavrushin, *Zh. Obshch. Khim.*, 1976, **17**, 691; (b) V. Orlov, I. Borovoi, U. Surov and V. F. Lavrushin, *Zh. Obshch. Khim.*, 1976, **46**, 2138; (c) A. Hoser, Z. Laluski and H. Maluszynska, *Acta Crystallogr., Sect. B: Struct. Crystallogr. Cryst. Chem.*, 1980, **36**, 1258.
- 10 (a) A. Saito, M. Umakoshi, N. Yagyu and Y. Hanzawa, *Org. Lett.*, 2008, **10**, 1783; (b) P. Wessig, C. Glombitza, G. Müller and J. Teubner, *J. Org. Chem.*, 2004, **69**, 7582; (c) Y. Wan, X. M. Chen, L. L. Pang, R. Ma, C. H. Yue, R. Yuan, W. Lin, R. Cheng Bo and H. Wu, *Synth. Commun.*, 2010, **40**, 2320; (d) C. Carrignon, P. Makowski, M. Antonietti and F. Goettman, *Tetrahedron Lett.*, 2009, **50**, 4833.
- 11 D. A. Thornton, *Coord. Chem. Rev.*, 1990, **104**, 173.
- 12 H. C. Brown, *J. Am. Chem. Soc.*, 1957, **22**, 339.
- 13 (a) M. L. Kantouri, T. Dimitriadis, C. D. Papadopoulos, M. G. Agnieszka Czapik and A. G. Hatzidimitriou, *Z. Anorg. Allg. Chem.*, 2009, **635**, 2185; (b) S. M. Cohen, M. Meyer and K. N. Raymond, *J. Am. Chem. Soc.*, 1998, **120**, 6277.
- 14 R. D. Hancock and D. A. Thornton, *Theor. Chim. Acta*, 1970, **18**, 67.
- 15 R. Seoudi, G. S. El-Bahy and Z. A. El Sayed, *Opt. Mater.*, 2006, **29**, 304–312.
- 16 (a) M. M. El-Nahass, M. M. Sallam and H. A. Ali, *Int. J. Mod. Phys. B*, 2005, **19**, 4057; (b) M. M. El-Nahass, K. F. Abd-El-Rahman and A. A. A. Darwish, *Mater. Chem. Phys.*, 2005, **92**, 185–189.
- 17 A. Thakur, G. Singh, G. S. S. Saini, N. Goyal and S. K. Tripathi, *Opt. Mater.*, 2007, **30**, 565.
- 18 S. Adachi, *Optical Properties of Crystalline and Amorphous Semiconductors*, Kluwer Academic Publishers, Boston, 1999.
- 19 G. M. Sheldrick, *Acta Crystallogr., Sect. A: Found. Crystallogr.*, 2008, **64**, 112.